

## **$q_{95}<2$ Operation Via Control of MHD Stability in the DIII-D Tokamak**

P. Piovesan<sup>1</sup>, J. Bialek<sup>2</sup>, J.M. Hanson<sup>2</sup>, R.J. La Haye<sup>3</sup>, M.J. Lanctot<sup>3</sup>, P. Martin<sup>1</sup>, G.A. Navratil<sup>2</sup>, M. Okabayashi<sup>4</sup>, C. Paz-Soldan<sup>3</sup>, E.J. Strait<sup>3</sup>, F. Turco<sup>2</sup>, P. Zanca<sup>1</sup>, M. Baruzzo<sup>1</sup>, T. Bolzonella<sup>1</sup>, A. Hyatt<sup>3</sup>, G.L. Jackson<sup>3</sup>, L. Marrelli<sup>1</sup>, L. Piron<sup>1</sup>, D. Shiraki<sup>2</sup>, A. Turnbull<sup>3</sup>

<sup>1</sup>*Consorzio RFX, EURATOM/ENEA Association, Padova 35127, Italy*

<sup>2</sup>*Columbia University, New York, NY 10027, USA*

<sup>3</sup>*General Atomics, PO Box 85608, San Diego, CA 92186-5608, USA*

<sup>4</sup>*Princeton Plasma Physics Laboratory, Princeton, NJ 08543-0451, USA*

In tokamaks the energy confinement time increases almost linearly with current,  $I_P$ , hence the interest to maximize it for given toroidal field,  $B_T$ . Since first experiments, though, a severe  $I_P$  limit at fixed  $B_T$  was found [1]. This is set by the external kink mode, which is unstable above a critical  $I_P/B_T$  ratio [2]. In terms of edge safety factor, this occurs at  $q(a)=aB_T/(RB_P)=2$ . Several experiments confirmed this limit with  $q_{95}$ , the relevant parameter in diverted tokamaks. If the wall resistivity is included, the external kink converts into a resistive-wall mode (RWM), its growth rate being reduced to  $1/\tau_w$ , the inverse wall penetration time, which allows its feedback control. Recently, this limit was overcome in RFX-mod run as a low- $I_P$ , circular tokamak by magnetic feedback control of the  $m=2/n=1$  RWM [3]. This motivated further experiments in a larger tokamak, which were performed in DIII-D and confirmed that the  $q_{95}=2$  limit can be overcome by MHD stability control.

Low- $q_{95}$  operation, even with  $q_{95}>2$ , requires careful design of the discharge setup, to avoid  $m>2/n=1$  external kinks that can grow as  $q_{95}$  decreases. Being driven by the edge current gradient, they can be avoided by keeping it low, e.g. by slowly ramping  $I_P$ . Fig. 1 shows a stable L-mode DIII-D discharge with  $q_{95}=2.2$  obtained by a slow  $I_P$  ramp. Also other aspects affecting stability were optimized. The shape was tailored to minimize the wall distance, to help passive MHD stability. NBI was added to spin-up the plasma and avoid tearing mode locking. Static  $n=1$  error fields (EF) were compensated with external coils by the compass-

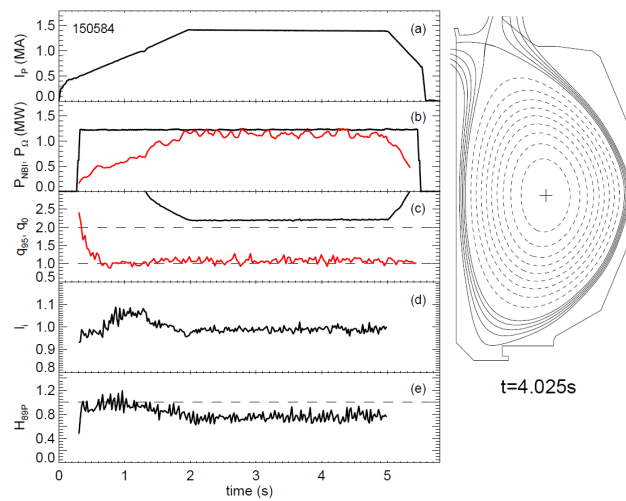


Figure 1. Main waveforms and shape of a  $q_{95}=2.2$  plasma. The figure consists of five vertically stacked time-series plots (a-e) and a plasma cross-section diagram. Plot (a) shows current  $I_P$  (MA) increasing from 0.2 to 1.1 over 5 seconds. Plot (b) shows NBI power  $P_{NBI}$  (MW) and ELM power  $P_{ELM}$  (MW) fluctuating around 1.0. Plot (c) shows the edge safety factor  $q_{E95}$  (red line) and its derivative  $dq_{E95}$  (black line) decreasing from 2.5 to 1.0. Plot (d) shows the magnetic field component  $B_\phi$  (Gauss) with a sharp initial drop. Plot (e) shows the magnetic field component  $H_{B95}$  (Gauss) with a sharp initial drop. To the right is a plasma cross-section at  $t=4.025s$  with field lines and a central island marked with a plus sign.

scan technique. These plasmas have regular sawtooth activity. The safety factor on-axis is close to 1 and the current profile does not significantly evolve during flattop, as indicated by the internal inductance in panel (d). The confinement performance, represented by the ratio between the measured energy confinement time and the L-mode 89P scaling in panel (e), is degraded by about 20% with respect to L-mode performance similar to [4].

After optimizing this very low- $q_{95}$  plasma, the  $I_p$ -ramp was prolonged to reach  $q_{95}<2$ . Fig. 2 compares the  $q_{95}=2.2$  plasma (black) and two such attempts. The case in red has no stability control and disrupts as  $q_{95}\approx 2$  due to the growth of an  $n=1$  mode. In the blue case, RWM feedback was turned on, using internal coils driven by audio-amplifiers. As a result,  $q_{95}$  is maintained below 2 for 0.45s,  $\sim 150\tau_w$ , much longer than the RWM growth time. Control is eventually lost due to voltage limits reached in the power supplies.

Confinement degradation up to 50% occurs as  $q_{95}<2.1$ , as shown in Fig. 2(d). However, it was not the aim of these first experiments to optimize confinement. A single attempt to obtain H-mode led to modest values of  $H_{89P}=1.5$  and  $\beta_N=1.1$ , which nonetheless results, thanks to the low  $q_{95}=1.95$ , in significant normalized fusion performance  $G=H_{89P}\beta_N/q_{95}^2=0.43$  [5]. Future work should focus on sustaining a  $q_{95}<2$  flattop and optimizing confinement, to evaluate the real benefits of low- $q_{95}$  operation on performance.

Fig. 3 shows  $I_i$  vs.  $q_{95}$  during flattop or before disruption for plasmas without (open symbols) and with RWM feedback (full symbols). Blue circles represent stable plasmas without feedback. RWM feedback allows access to  $q_{95}<2$  for periods much longer than  $\tau_w$ . All plasmas reaching  $q_{95}<2.2$  disrupt due to an  $n=1$  RWM, with growth time of a few ms. In the cases in red, the  $n=1$  mode is preceded by an  $n=2$  tearing mode that locks, reducing the edge

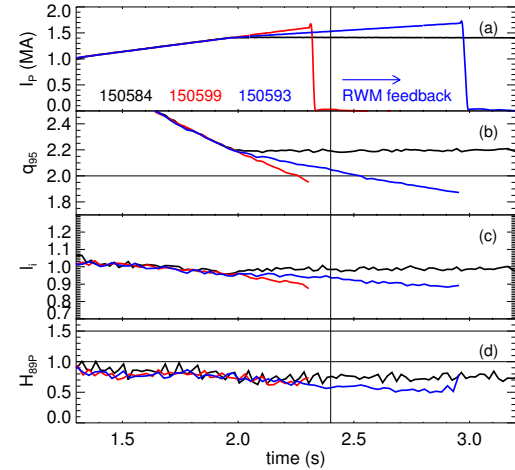


Figure 2. Reference  $q_{95}=2.2$  discharge compared with two attempts to  $q_{95}<2$  without (red) and with RWM feedback (blue).

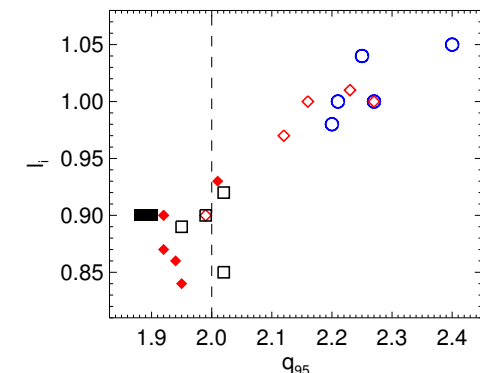


Figure 3.  $I_i$  vs  $q_{95}$  for all available discharges. Symbols explained in the text.

rotation. Compensation of  $n=2$  EF may help to avoid these events. No 2/1 tearing mode is observed, even if it may be expected to be an issue at low  $q_{95}$ .

Fig. 4 shows the growth of an  $n=1$  mode compatible with a RWM. It shows the  $n=1$   $B_p$  amplitude and phase as  $q_{95}$  approaches 2. The  $n=1$   $B_p$  increases as the instability threshold is approached, likely due to resonant field amplification of an EF [6]. As  $q_{95} \approx 2$ , an  $n=1$  mode grows with  $\gamma \approx 1/\tau_w$ , as expected for a RWM. The  $n=1$  mode spatial structure in panel (f) is compatible with VALEN ideal MHD stability simulations (not shown here).

Fig. 5 analyzes the RWM feedback dynamics and what causes its failure. The  $n=1$   $B_p$  amplitude increases after sawtooth crashes, due to  $n=1$  postursors rotating at few kHz. RWM feedback is not effective on these time scales, its bandwidth being limited to a few 100Hz. Panel (c) compares the  $n=1$  I-coil (black) and the  $n=1$   $B_p$  amplitudes filtered below 300Hz (red). A good match can be noted. These amplitudes vary on different time scales: (i) a slowly increasing component with almost constant phase likely due to an EF; (ii) a transient increase of the  $n=1$  plasma response after sawteeth, with almost constant phase, not due to  $n=1$  postursors that are filtered out, but likely to a transient response to the EF; (iii) a faster time scale associated with  $n=1$  mode rotation at a few 100Hz. This is likely induced by feedback, being present only at high enough gain. Feedback does not fully suppress the RWM, but it maintains it at finite, low amplitude. This is likely due to an uncompensated EF, but also to mode rotation. To follow the rotating mode,

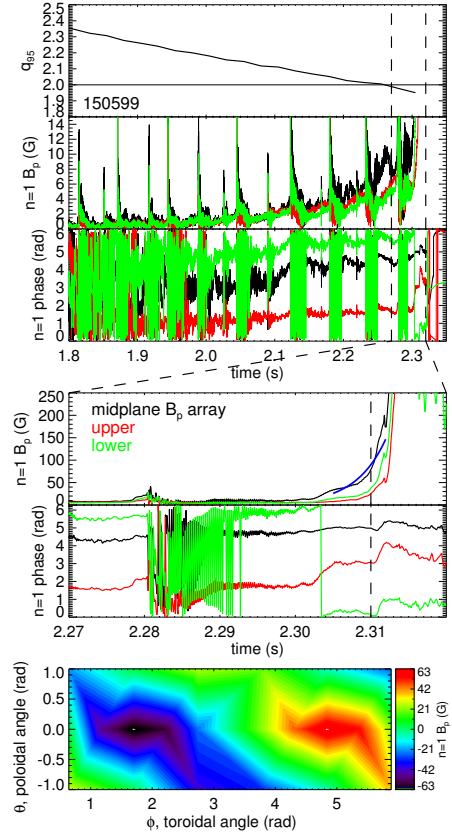


Figure 4.  $B_p$   $n=1$  amplitude and phase as  $q_{95}$  approaches 2 and at the RWM onset.

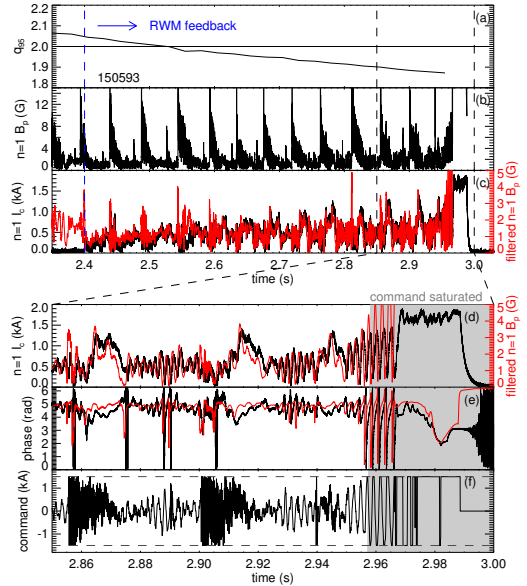


Figure 5. RWM feedback dynamics.

feedback increases the current request, which eventually saturates. As a result, control is lost and disruption follows. This is thus due to a technical limit, not to a physical one.

To interpret these results and improve RWM control, a simple model developed for RFX-mod was used [3]. This is a cylindrical, linear MHD model of the RWM, including a uniform resistive wall, active coils, finite bandwidth amplifiers, and discrete feedback logic. The model parameters (RWM  $\gamma$ , bandwidth, latency) are set to their experimental values. A periodic  $n=1$  EF pulse is added to mimic sawteeth. With these inputs full RWM suppression and no mode rotation are predicted.

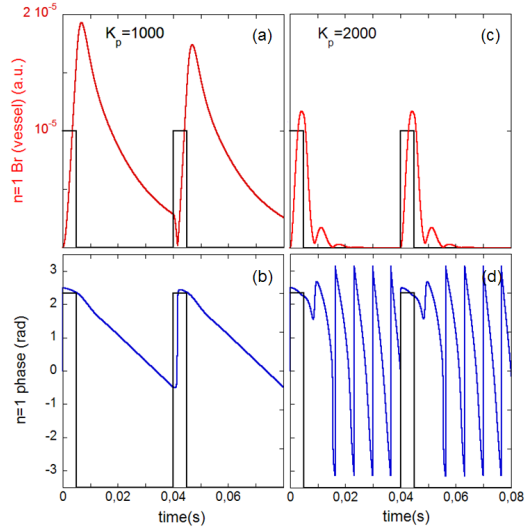


Figure 6. Simulations of RWM feedback.

The only way to have mode rotation is to add a small error in the  $n=1$  phase. This may be due to imperfect match between mode and coils, or to delays due to wall screening. Fig. 6 shows two simulations at different proportional gain with 7.5deg error. At higher gain, feedback reduces the mode faster, but it also induces rotation at a frequency similar to the experiment. A phase error could be easily compensated in the experiment. In this case, the model would predict RWM stabilization and much lower current request.

The first  $q_{95}<2$  operation of a large, D-shaped tokamak was obtained in DIII-D by MHD stability control. Even if these results are limited to L-mode and RWM control needs to be optimized, no intrinsic physics limits to  $q_{95}<2$  operation were found, which opens an interesting perspective for this new operation. Moreover, even without effort to confinement optimization, initial H-mode results indicated promising fusion performance.

*Acknowledgement.* This work was done within the DIII-D experimental time dedicated to the 2012 Torkil Jensen Award and was supported by the US Department of Energy under DE-FC02-04ER54698, DE-FG02-04ER54761, and DE-AC02-09CH11466, as well as by the European Communities under the contract of Association between EURATOM/ENEA. The views and opinions expressed herein do not necessarily reflect those of the European Commission.

- [1] E.J. Strait *et al.*, Plasma Physics and Controlled Nuclear Fusion Research 1988: Proc. 12th Int. Conf. Nice, 1988 (IAEA, Vienna, 1988), Vol. 1; J.A. Wesson *et al.*, Nucl. Fusion **29**, 641 (1989); E. Lazzaro *et al.*, Nucl. Fusion **20**, 2157 (1990); Y. Kamada *et al.*, Nucl. Fusion **33**, 225 (1993).
- [2] M.S. Chu and M. Okabayashi, PPCF **52**, 123001 (2010).
- [3] P. Zanca *et al.*, PPCF **54**, 094004 (2012); M. Baruzzo *et al.*, Nucl. Fusion **52**, 103001 (2012).
- [4] D.P. Schissel *et al.*, Nucl. Fusion **32**, 107 (1992).
- [5] T.C. Luce *et al.*, Phys. Plasmas **11**, 2627 (2004).
- [6] A.H. Boozer, Phys. Rev. Lett. **86**, 5059 (2001).